JBC Papers in Press. Published on May 1, 2020 as Manuscript RA119.012348
The latest version is at https://www.jbc.org/cgi/doi/10.1074/jbc.RA119.012348

Native nanodiscs formed by styrene maleic acid copolymer derivatives help recover infectious prion multimers bound to brain-derived lipids

Mansoore Esmaili[1], Brian P. Tancowny[1,2], Xiongyao Wang[1,2], Audric Moses[3], Leonardo Cortez[2,4], Valerie Sim[2,4], Holger Wille[1,2*], Michael Overduin[1*]

From the [1] Department of Biochemistry, University of Alberta, Edmonton, Alberta T6G 2H7, Canada; [2] Centre for Prions and Protein Folding Diseases, University of Alberta, Edmonton, Alberta T6G 2M8, Canada; [3]Lipidomics Core Facility, Faculty of Medicine and Dentistry, University of Alberta, Edmonton, Alberta T6G 2H5, Canada; [4]Division of Neurology, Department of Medicine, Centre for Prions and Protein Folding Diseases, and Neuroscience and Mental Health Institute, University of Alberta, Edmonton, Alberta, Canada T6G 2M8.

Running title: Native nanodiscs resolve infectious lipid-prion multimers

[*] To whom correspondence should be addressed: Michael Overduin, Department of Biochemistry, University of Alberta, Edmonton, Alberta T6G 2H7, Canada, overduin@ualberta.ca; Tel.: +1-780-492-3518; FAX: +1 780 492 0886; or Holger Wille, Department of Biochemistry, University of Alberta, Edmonton, Alberta T6G 2H7, Canada, wille@ualberta.ca; Tel.: +1-780-248-1712; FAX: +1 780 492 0886

Keywords: membrane protein, native nanodiscs, prion, protein misfolding, styrene maleic acid (SMA) copolymer, styrene-maleic acid lipid particle (SMALP), neurodegenerative disease, lipid-protein interaction, protein aggregate

ABSTRACT

Prions are lipidated proteins that interact with endogenous lipids and metal ions. They also assemble into multimers and propagate into the infectious scrapie form known as PrP^{Sc}. The high-resolution structure of the infectious PrP^{Sc} state remains unknown and its analysis largely relies on detergent-based preparations devoid of endogenous ligands. Here we designed polymers that allow isolation of endogenous membrane:protein assemblies in native nanodiscs without exposure to conventional detergents that destabilize protein structures and induce fibrillization. A set of styrene-maleic acid (SMA) polymers including a methylamine (MA) derivative facilitated gentle release of the infectious complexes for resolution of multimers, and a thiol-containing version promoted crystallization. Polymer extraction from brain homogenates from Syrian hamsters infected with Hyper prions and wild-type mice infected with Rocky Mountain Laboratories (RML) prions yielded infectious prion nanoparticles including oligomers and microfilaments bound to lipid vesicles. Lipid analysis revealed the brain phospholipids that associate with prion protofilaments as well as those that are specifically enriched in prion assemblies captured by the MA-modified copolymer. A comparison of the infectivity of PrP^{Sc} attached to SMA lipid particles (SMALPs) in mice and hamsters indicated that these amphipathic polymers offer a valuable tool for high-yield production of intact, detergent-free prions that retain *in vivo* activity. This native prion isolation method provides an avenue for producing relevant prion:lipid targets and potentially other proteins that form multimeric assemblies and fibrils on membranes.

Neurodegenerative diseases, including Alzheimer's disease, Parkinson's disease and transmissible spongiform encephalopathies, involve pliable membrane-associated proteins that adopt multiple conformational states. The critical role of the membrane is a confounding variable in mechanistic studies of these systems. Bound lipids are typically lost during membrane

Downloaded from http://www.jbc.org/ at University of Alberta Libraries on May 28, 2020

protein separation with detergents. This can lead to deleterious artifacts as these lipids usually stabilize otherwise labile structures and modulate sensitive functions (1). Preserving the relevant target state is important for developing accurate diagnostic assays and therapeutic agents, which are growing priorities given the rising incidence and impacts of these neurodegenerative conditions (2,3). There is a particular need to find alternatives for presenting and studying prions due to the complexity of their states including monomers, multimers, protofibrils and fibrils that are modulated by various modifications, ligands, detergents, and surfaces. Native nanodiscs are increasingly used to prepare assemblies of endogenous membrane:protein assemblies ("memteins") with lipid ligands and post-translational modifications in their biologically intact states (1), but have limitations including excessive negative charge and polydispersity. Moreover, they have not yet been used to tackle prions. Here, SMA copolymer derivatives optimized for stabilizing and isolating memteins were developed to address the challenges presented by transient lipid-bound infectious prion multimers.

Prions are normally associated with membranes through GPI anchors, although their endogenous lipid complement is unclear. Prion analysis has relied on maintaining high concentrations of conventional detergents such as sarkosyl (4,5), despite induced alterations of structural properties (6), compromised interactions with physiological partners including heparin (7), and fibrilization of prions including Proteinase K (PK)- and phosphotungstic acid (PTA)-treated RML strain-infected mouse brain homogenates (8). These studies prevail due to the lack of milder substitutes that could more gently release intact prion:lipid assemblies for analysis (9). Addressing this limitation could lead to resolving the structural identities of the infectious prion forms and the mechanisms underlying their toxicity, lipid perturbations (10-13), GPI-anchoring and PK-sensitive oligomerization during prion propagation (14,15). Towards this end, we have developed and tested a series of SMA polymers for the detergent-free isolation of infectious prions in native nanodiscs. These are used for *in vitro* structural and *in vivo* infectivity assays of protease-resistant prion (PrP^{res}) assemblies from the brains of Hyper strain-infected hamsters and RML strain-infected FVB mice.

A custom polymer was designed to overcome anticipated challenges with prions. Amphipathic polymers that contain statistical distributions of styrene and maleic acid monomers in non-alternating ratios are known to insert into virtually any cellular membrane for spontaneous formation of native nanodiscs (16-18). However, the heterogeneity of their sequences precludes atomic resolution of the polymers or bound lipid headgroups in 3D structures (19,20). Alternating polymers are more homogenous due to their regular 1:1 repeating pattern of styrene and maleic acid subunits but are relatively ineffectual at membrane solubilization (21-23). To synthesize alternating SMA(1:1) derivatives, which are more homodispersed and better suited to solubilizing metal-dependent proteins, including prions, we used less charged maleimide groups rather than maleic acid groups. Clusters of lipid-inserting styrenes can also mediate undesirable nonspecific interactions with fibrils, and hence the styrene ratio was halved with a compensatory methyl added onto the maleimide. Crystallization and structural analysis would benefit from more regularized belts of polymer around nanodiscs that encapsulate protein-phospholipid complexes. Hence, we incorporated thiol groups to offer hydrogen bonding and crosslinking potential. This SMA series is optimized for prions but has broad implications for biochemical, structural and lipidomic analyses of diverse membrane proteins, many of which remain intractable (24). Here, we investigated the strengths and weaknesses of different formulations of SMA copolymers *in vivo* and *in vitro* applications as alternatives for detergents for resolving infectious prions, with potential applicability to virtually any membrane-associated target.

Results

Comparison of SMA copolymers

A series of four SMA copolymers was synthesized to contrast the effects of polymer charge, hydrophobicity and reactivity on native prion solubilization and activity. The SMA(2:1) and SMA(3:1) copolymers contain non-alternating sequences with 2:1 and 3:1 ratios of

Downloaded from http://www.jbc.org/ at University of Alberta Libraries on May 28, 2020

styrene to maleic acid monomers, respectively, and offer distinct membrane interaction and solubilization profiles. They were activated by alkaline hydrolysis of the respective styrene-maleic anhydride forms (Fig. 1a) for subsequent analysis of prion solubilization and activity. A derivative with free thiol groups was synthesized from SMA polymer by grafting cysteamine to SMA(2:1) polymer (Fig. 1b), with the thiol groups in the resulting SMA-SH polymer (16) offering handles for cross-linking. A methylamine derivative termed "SMA(1:1)ma" was synthesized that offers an equimolar ratio of comonomers (Fig. 1c), less charge and hence increased in predicted polycation compatibility, and alternating hydrophobic subunits for greater homogeneity and potential for structural resolution.

Before proceeding to the solubilization of prions from the mammalian brain, we compared the abilities of the various polymers to solubilize multilayer vesicles (MLVs) composed of dimyristoyl phosphatidylcholine (DMPC) lipid. The SMA(1:1)ma form was able to solubilize membranes at a concentration of 1%, which is similar to conventional non-alternating SMA polymers, despite having a lower amount membrane-binding styrene groups. This was expected due to the alkylamine derivatization reducing the net negative charge and increasing the overall polymer hydrophobicity, which is needed for efficient membrane insertion. Membranes were solubilized by SMA(1:1)ma at up to 10 mM calcium chloride, while SMA(2:1) precipitates above 5 mM; SMA(1:1) is active from pH 5 to 10 (Fig. S1), while other SMA polymers have narrower pH ranges and are optimal at pH 8. Thus SMA(1:1)ma has a broader solution compatibility, reduced charge, sufficient hydrophobicity as well as lower sequence heterogeneity while retaining comparable membrane solubilization activity. Hence it was included in our polymer panel to solubilize native-state prion particles.

Isolation and partial purification of infectious PrP (PrP^{Sc}) using SMALP.

Like established prion purification methods, the SMA-based approach also utilizes PTA to bind PrP^{Sc} assemblies and separate them from other brain components (8). Optimization of the SMA protocol to achieve high recovery of multimeric PrP^{Sc} reduced the duration of the incubation with PTA to one hour. Unlike detergents that need to be maintained throughout the protocol, a minimal concentration of SMA polymer (1% w/v) was added only during the initial incubation with brain homogenate (Fig. S2) to reduce the heterogeneity of nanodiscs for fractionation and TEM imaging. Due to the stability of the nanodiscs, no further polymer needed to be added downstream of the initial solubilization.

Resistance to proteolytic digestion is a hallmark of many prion strains found in tissues of organisms exhibiting transmissible spongiform encephalopathies. Both Proteinase K and Pronase E were used, as the latter retains the GPI-anchoring needed for stable membrane interactions of prions (25). Either protease could be used to prepare PrP^{Sc} from brain homogenate with similar results. However, yield of PrP^{Sc} filaments in electron micrographs from Pronase E-treated samples was noticeably higher. Consequently, the Pronase E-resistant prion (hence PrP^{Sc}) was prioritized for preparation of membrane:prion assemblies in native SMA nanodiscs.

Native prion proteins are variably glycosylated and are present as three characteristic bands on immunoblots, corresponding to diglycosylated, monoglycosylated, and unglycosylated forms. All SMA-isolated PrP^{Sc} samples, whether isolated from Hyper strain-infected hamsters or RML strain-infected mice, share a similar profile of glycoforms with distinct molecular weights that match those of sarkosyl-purified PrP^{Sc} samples (Fig. 2b, 2c). However, the purity of PrP^{Sc} extracts, as well as their physical appearances, differed between the various SMA-purified samples (Fig. S2). Prions solubilized by SMA(2:1) treatment were the least turbid, whereas SMA(1:1)ma-purified prions appeared as a brown waxy pellet, which suggested the inclusion of more lipid or heme-containing proteins such as ferritin or cytoskeletal proteins like keratin (Fig. S2) (26). Despite the use of benzonase nuclease (18) and high-speed centrifugation of all samples before the gel electrophoresis, high molecular weight aggregates appeared in both SMA(1:1)ma and

Downloaded from http://www.jbc.org/ at University of Alberta Libraries on May 28, 2020

SMA(2:1) preparations. Immunoblotting experiments confirmed that the size of aggregates does not correlate with PrP^{Sc} (data not shown). Due to the presence of apparent keratin fibers in EM images, we attributed the high molecular weight aggregates to cytoskeletal protein fibers.

Given the milder membrane solubilization provided by SMA polymers, we speculated that more prion multimers might be retained. The distribution of low-density SMA-purified PrP^{Sc} complexes from hamster and mouse strains was examined via equilibrium sedimentation in step-wise sucrose density ultracentrifugations (Fig. 3). The majority of PrP^{Sc} protein extracted by SMA from Hyper-infected hamsters was buoyant and found in the top fraction, and hence represented lipid-associated states, while the levels of dense aggregates that sedimented to the bottom of the gradient was relatively insignificant. The SMA(1:1)ma treatment of PrP^{Sc} derived from brains of the Hyper (HY) strain showed a distribution of oligomeric states that migrated faster in the sedimentation three-step sucrose gradients than complexes obtained with the other SMAs. Together the migration behavior in the sucrose gradients indicates that the various SMA polymers preferentially solubilize the lipid:prion complexes.

Transmission electron microscopy of SMALP-isolated PrP^{Sc}

We investigated the morphology of the prion fibrils that were obtained by SMA extraction from the brain. The SMA isolates of PrP^{Sc} contain mainly two protofilaments that have diameters of approximately 20 nm in negative stain electron microscopy images (Fig. 4), while entangled long rods were seen in sarkosyl-treated samples. Moreover, lipid vesicles were found in PrP^{Sc} preparations obtained with SMA and are particularly enriched in SMA(1:1)ma isolates, which show protofilament: vesicle complexes. The lipid vesicles can be removed by treatment of SMA-PrP^{Sc} preparations with polyethylene glycol (PEG)6000 (4% w/v, 4 °C, overnight), which precipitates the PrP^{Sc} for EM analysis as relatively homogenous protein fibrils. Large discs with diameters of 45 ± 5 nm containing 2D crystals of PrP^{Sc} can be obtained from PK- and SMA-SH treated Hyper strain brains (Fig. 5a), and are strongly reminiscent of those seen in earlier studies (27-29). The available thiols of SMA-SH and the higher prion yield from prion-infected hamster samples may both contribute to the formation of these PrP^{Sc} 2D crystals, which were rarely seen in other SMA brain isolates. The top fractions of the sucrose gradients of SMA(2:1)- and SMA(1:1)ma HY PrP^{Sc} contain fibrils within the low-density lipid raft microdomains, which is consistent with native PrP^{Sc} fibril association with the plasma membrane (Fig. 5b,c).

Lipid profile of the infectious PrP^{Sc} in SMALPs versus sarkosyl

Co-purified lipids of PrP^{Sc} are also key for the biological transformation of cellular PrP to the scrapie isoform (11,13,30,31). Unlike some detergents that dissociate protein-bound lipids, SMA polymers have been shown to be useful tools for studies of lipids bound to membrane proteins (32) and amyloids (14,33). In this regard, however, the use of detergents and the infectivity associated with high titer PrP^{Sc} pellets have limited the investigation of the lipid profile of infectious prions from endogenous sources (34). The lipids associated with PrP^{Sc} assemblies extracted from brains of infected and healthy hamsters and mice were identified and quantified, allowing relative levels of eleven types of lipid to be compared (Fig. 6). Using an internal standard (batyl alcohol) added to the sample during lipid extraction, the amount of each lipid was determined by HPLC (data not shown). The findings demonstrate that SMA(1:1)ma discs provide the highest capacity for isolation of various types of lipids, a finding which is in accordance with the waxy appearance of PrP^{Sc} pellet purified using this polymer. The next highest prion-associated lipid capacity are offered by SMA(2:1) and SMA-SH polymers, respectively. Interestingly, HY hamster and RML strains have a relatively distinctive lipid profile; for instance, triglyceride (TG) is solely present in HY hamster samples. The lipid profiles also reveal the presence of critical signaling lipids including cholesterol, phosphatidylinositol (PI) and sphingomyelin (35) in close proximity to PrP^{Sc} molecules. This is consistent with reports of

Downloaded from http://www.jbc.org/ at University of Alberta Libraries on May 28, 2020

other misfolding diseases such as Alzheimer's disease and type 2-diabetes (36,37).

Bioassay of SMALP- PrP^{Sc} particles

The symptoms of mice and hamsters inoculated with PrP^{Sc} extracted from brain with different SMA polymers or sarkosyl were compared to those inoculated with brain homogenate from infected animals (Table 1). Prion disease presents as ataxia, scruffy coats, loss of gait, weight loss and head bobbing at the time of euthanasia (38). The average incubation times from SMALP-PrP^{Sc} particle inoculation until terminal disease was consistently around 85-90 days in Hyper hamsters, with SMA(1:1)ma, SMA(2:1) and SMA-SH-purified PrP^{Sc} showing similar periods (Table 1a) as sarkosyl purified PrP^{Sc}. In contrast, inoculation with SMA(3:1)-purified PrP^{Sc} yielded the longest incubation times. As expected, inoculation with 1% prion 263K brain homogenate from infected animals was most efficient. Given the 153 days for average incubation time of RML prions in FVB mice, mice incubated with SMA-SH and SMA(3:1) purified PrP^{Sc} showed the shortest and longest incubation times, i.e. 163 and 187 days, respectively (Table 1b). Despite the variability of incubation period for different SMA-purified samples, animals in SMA(3:1), SMA(2:1), SMA(1:1)-methylamine and SMA-SH groups show the same clinical symptoms, suggesting that the isolation method did not alter prion strain characteristics. Brain homogenates of animals infected with isolated SMALP-PrP^{Sc} particles were used for a second passage into healthy hamsters (Table 2). The incubation periods display, to a great extent, the same trend in both incubation period and symptoms at terminal stage as first passage, with SMA(3:1) having the longest incubation periods. Protease digestion of postmortem brain tissues reveals that all animals, regardless of the incubation period and clinical symptoms, display the characteristic profile of PK-resistant PrP (Fig. S3), again supporting our conclusion that each purification protocol did not alter the strain characteristics.

Discussion

We have shown that infectious membrane-associated prions can be directly isolated intact from rodent brains using custom SMA copolymers, providing a viable route to prepare one of the most challenging complexes with no exposure to detergent and minimal use of PTA or added polymer. The density-based fractionation of the resulting particles yields the lipid-bound state of PrP^{Sc} protofilaments with least aggregation (8) and multimers that co-purify with SMALP-nanodiscs.

The choice of protease is a key element in the isolation of non-fibrillar, membrane-bound and infectious PrP^{Sc}. To this end, the copolymer based strategy in combination with high-performance proteases such as thermolysin (39) could yield a gentle and minimal perturbing preparative approach for further structural analysis. Our data shows that the SMALP system is compatible with proteases such as PK and PE for isolation of truncated and intact PrP^{Sc} assemblies, respectively. Structural investigation of GPI anchor-dependent propagation of PrP^{Sc} and hence its lipid raft related signaling would require the intact native assemblies of PrP^{Sc}-lipids and to this date the amphipathic polymers are the only available tools for this purpose (40). This discovery that SMA(1:1)ma is particularly effective at intact membrane:prion isolation provides an avenue for production of nanodiscs with reduced nonspecific interactions, polydispersity and calcium sensitivity and thus overcomes multiple limitations of other SMA polymers. The notable increase in 2D crystals that resulted from the PrP^{Sc} solubilization with SMA-SH demonstrated its utility as a tool for the structural characterization of PrP^{Sc} in the form of non-fibrillar assemblies (27-29).

Demonstration of the solubilization of the biologically active multimer prion protein with SMA(1:1)ma with a two-fold improvement in tolerance to cation and membrane binding capacity indicates wider utility for diverse memteins that are often cation and lipid dependent. The advantages of SMA(1:1)ma indicate significant potential for lipidomic and metabolomic analyses of membrane assemblies including high-titer PrP^{Sc} complexes from infected organisms. Such polymers provide an advantage over conventional detergents which dissociate physiologically important lipid molecules or ligands, except those which are tightly bound and buried between core fibers, such as the unresolved hydrophobic ligands in

Downloaded from http://www.jbc.org/ at University of Alberta Libraries on May 28, 2020

structures of tau fibers (41). Determination of ligand identities and quantification of bound lipids allows analysis of the native membrane environment and enables mechanistic studies of the lipid-dependent transformation of prions from the normal cellular state to the scrapie form. This analysis will rely on fractionation and time-resolved studies of the SMA-treated brain homogenate. This separation of transient and irreversible states could be facilitated by differences in their hydrodynamic sizes and conformations, which we speculate could be lipid-dependent. Stabilization and resolution of the intermediate state most critical for infectivity is becoming increasingly feasible with the SMA derivatives presented here. In addition other solutions may be developed, with cellulose ethers and methylcellulose having been shown to prolong the incubation periods of PrP^{Sc} in prion disease animal models (42), providing a broader context for the use of polymers to stabilize and study critical prion states.

In addition to their utility for *in vitro* structural and lipid-binding studies of membrane proteins, SMA polymers have *in vivo* applications as drug delivery vehicles (43,44). Here we used a polymer concentration of ~1% w/v to prepare prion nanoparticles for structural and infectivity studies, although even lower concentrations (0.5% w/v) are also effective in liberating the PrP-lipid complexes. As the prion-containing SMALP was added to brain homogenate in only one initial step, the purified PrP^{Sc}-lipid assembly was injected into animals with little if any free SMA polymer present. The incubation periods of SMA-purified PrP^{Sc} strains can be explained in light of previous studies on the anti-prion activity of dendrimers (45), which suggest that polymer surface charge does not correlate with the mechanism of action of these polymers, including prolonging of the incubation time of PrP^{Sc}. Moreover, several studies confirmed that low toxicity polymers can disaggregate PrP^{Sc} polymers, thus giving rise to longer incubation times in murine models (46-48). The application of SMA(1:1)ma would reduce the net charge and hydrophobic clusters of copolymers and nanoparticles, thus allowing specific target interactions to be favoured over non-specific electrostatic and hydrophobic interactions. Hence the SMA derivative polymers presented here could offer insights and utility for structural biology, drug discovery and delivery applications for a wide array of memtein targets.

Experimental Procedures

Polymer Synthesis. SMA(2:1) and SMA(3:1) (Polyscope) were each modified from the anhydride version to their corresponding acid forms by hydrolysis in 1M NaOH while refluxing at 70 °C for 3 hours (14) and dried under vacuum. A cysteamine-grafted derivative of SMA(2:1) (SMA-SH) was synthesized using established methods (49) and stored with 5 mM dithiothreitol (DTT). SMA(1:1)ma was synthesized from SMA(1:1) as described in **Fig. 1**. Stock solutions (8% w/v, pH 7.5) of each polymer were prepared in Dulbecco's phosphate-buffered saline (DPBS) with 5% glycerol (v/v), Fourier Transform InfraRed (FTIR) spectra were collected (data not shown) and samples were stored frozen until use.

Prion Isolation from Brains. Brain homogenates (20% w/v) were generated from clinically ill Hyper strain-infected Syrian hamster brains and RML-infected FVB mouse brains and prepared in DPBS+5% glycerol, mixed with 8% (w/v) SMA stock solution to a final concentration of 1% (w/v) and Pronase E (Sigma). Each mixture was then incubated at 37°C for 30 min after which the protease was inactivated by EDTA addition (50). Sodium phosphotungstic acid (PTA, 200 µL of 10% w/v, pH 7.2) was added and the mixtures were incubated for one hour at 37°C. The solutions were centrifuged at 16,500×g, and the pellets were re-suspended in DPBS and 5% (v/v) glycerol and stored at -20°C for later assays.

Equilibrium Sucrose Ultracentrifugation. Sucrose gradients in DPBS were prepared in 3.5 mL Beckman ultracentrifuge tubes in order to resolve prion multimers. Three independent sets of SMA-purified samples were overlaid on top of each gradient and spun at 130,000×g in a SWTi55 swinging-bucket rotor (Beckman Coulter) for at least 17 hours at 4°C. Fractions (200 µL) were collected from the top to the bottom of tubes and 40 µL aliquots were mixed with an equal volume of sample buffer (Bio-Rad) and heated for 10 min at 100°C as per Western blotting and SDS-PAGE gels.

Downloaded from http://www.jbc.org/ at University of Alberta Libraries on May 28, 2020

Negative-stain Transmission Electron Microscopy. Carbon coated copper grids (400 mesh) were charged using an EMS Pelco Easy Glow 100 x glow discharge unit (Ted Pella Inc, USA) for 30 seconds. Microliter amounts of each SMA-purified prion sample were loaded on the grids and adsorbed for 30 seconds. The grids were washed three times (3×50 µL) with ammonium acetate (100 mM and 10 mM, pH 6.8), and stained with filtered 2% uranyl acetate. Excess dye was removed using a filter paper and the grid was air-dried for at least 5 minutes before TEM imaging. Micrographs were collected using a Tecnai G20 transmission electron microscope equipped with an Eagle 4 k × 4 k CCD camera (FEI Company) using an acceleration voltage of 200 kV.

Infectivity assays. FVB mice were obtained by in-house breeding and 23 day old golden Syrian hamsters were purchased from Envigo. The SMA-isolated PrP^{Sc} samples and controls were serially diluted 100 times in DPBS and normalized by volume to brain equivalent. Likewise, brain homogenates of infected animals were subsequently used for the second passage. Diluted samples were then used to intracerebrally inoculate three independent groups, each with four animals, of healthy FVB mice (30 µL per animal) and/or Syrian hamsters (50 µL per animal). Their behavior was monitored on a daily basis and after clinical diagnosis of prion disease the brains of euthanized animals were isolated and stored at -80°C for analysis. Infectivity data were analyzed by SigmaPlot 14.0.

Immunoblotting and Silver Staining. Prion samples were mixed with an equal volume of 2× sample buffer containing 700 µM β-mercaptoethanol, and heated at 100 °C for 10 min. Before loading on pre-cast 10 or 12% stain-free SDS-PAGE gels (Bio-Rad) samples were centrifuged for 2 min at 14,000×g. Electrophoresis was performed at 100 V for ~ 2 hours at room temperature. Proteins were electrotransferred to polyvinylidene difluoride (PVDF) membranes (Millipore) at 100 volts for one hour at room temperature in 25 mM Tris pH 8.3, 192 mM glycine, 20% methanol (v/v). Membranes were blocked in tris buffered saline (TBS) with 0.1% (v/v) Tween and 5% (w/v) bovine serum albumin (BSA) for one hour at room temperature, followed by incubation overnight at 4°C with an in-house mouse anti-prion antibody. The membrane was washed three times for 10 minutes in TBS with 0.1% Tween, and further incubated with a secondary alkaline phosphatase (AP)-conjugated goat-anti-mouse antibody (Bio-Rad) for one hour. After three 10-minute washes, the membrane was incubated with 1 mL of AP-Substrate (Bio-Rad) and immunoblots were imaged using ImageQuant (GE Life Science).

Proteinase K Resistance Assay. The brain tissue of each infected animal was removed post-mortem, and a brain homogenate (10% w/v) was prepared in DPBS with 5% glycerol. To assess prion protease sensitivity, 160 µL of 10% brain homogenate was incubated with varying concentrations of PK (0, 5, 50, 200 µg/mL) at 37°C for 60 minutes with constant agitation. PK was inactivated by adding 0.5 mM phenylmethylsulfonyl fluoride (PMSF) and samples were mixed with 2 × sample buffer, heated to 100 °C, run on SDS-PAGE and immunoblotted using an anti-prion antibody. Silver staining methods (29) included fixing and washing gels in ethanol to remove excess SDS. After treatment with Farmer's reducer (0.05% sodium carbonate, 0.15% potassium hexacyanoferrate (III) and 0.3% sodium thiosulfate), gels were incubated with $AgNO_3$ for 20 minutes and developed in formaldehyde sodium carbonate solution.

Lipid Analysis. The total lipid was isolated from high titer PTA complexes of PrP^{Sc} solubilized in SMA polymer or sarkosyl according to established methods (51) using methanol:chloroform (1:2 v/v) in a BSL-2 lab biosafety cabinet following decontamination by incubation of PTA pellets with 5M guanidinium thiocyanate for one hour at room temperature (52). Total lipids were analyzed by HPLC based on (53), lipid classes were identified according to their retention time and comparison to commercial standards, and the amounts were quantified using calibration curves for each lipid class.

Downloaded from http://www.jbc.org/ at University of Alberta Libraries on May 28, 2020

Data Availability
All data are contained within the manuscript including the supplementary information.

Acknowledgements
We thank Claudia Acevedo-Morantes for assistance with electron microscopy, Xinli Tang for providing a primary anti-prion antibody. This work was supported by Alberta Prion Research Institute (APRI) Exploration (201600018), NSERC Discovery Grant (RGPIN-2018-04994) and Campus Alberta Innovates Program (#RCP-12-002C) grants to M.O. and an APRI Team Program award (201600029) to H.W.

Conflict of Interest
M.O. and M.E. have filed a patent on related SMA derivative copolymers and methods.

Ethics Statement
All experiments in mice and Syrian hamsters were performed in accordance with guidelines set by the Canadian Council on Animal Care and approved by the animal care use committee for Health Sciences 2 at the University of Alberta (protocol AUP00000884).

Author Contribution
HW, ME and MO designed the project and experiments. ME, BT, XW and AM performed experiments. ME, HW and MO wrote the manuscript. ME, AM, LC, VS, HW, and MO edited and critically provided input on the manuscript. MO and HW secured funding.

Downloaded from http://www.jbc.org/ at University of Alberta Libraries on May 28, 2020

REFERENCES

1. Overduin, M., and Esmaili, M. (2019) Memtein: The fundamental unit of membrane-protein structure and function. *Chem. Phys. Lipids* **218**, 73-84
2. Chiti, F., and Dobson, C. M. (2006) Protein misfolding, functional amyloid, and human disease. *Annu. Rev. Biochem* **75**, 333-366
3. Giles, K., Woerman, A. L., Berry, D. B., and Prusiner, S. B. (2017) Bioassays and Inactivation of Prions. *Cold Spring Harbor perspectives in biology* **9**, DOI:10.1101/cshperspect.a023499.
4. McKinley, M. P., Taraboulos, A., Kenaga, L., Serban, D., Stieber, A., DeArmond, S. J., Prusiner, S. B., and Gonatas, N. (1991) Ultrastructural localization of scrapie prion proteins in cytoplasmic vesicles of infected cultured cells. *Laboratory investigation; a journal of technical methods and pathology* **65**, 622-630
5. Riesner, D. (2003) Biochemistry and structure of PrP(C) and PrP(Sc). *Br Med Bull* **66**, 21-33
6. Breyer, J., Wemheuer, W. M., Wrede, A., Graham, C., Benestad, S. L., Brenig, B., Richt, J. A., and Schulz-Schaeffer, W. J. (2012) Detergents modify proteinase K resistance of PrP Sc in different transmissible spongiform encephalopathies (TSEs). *Vet Microbiol* **157**, 23-31
7. Shaked, Y., Engelstein, R., and Gabizon, R. (2002) The binding of prion proteins to serum components is affected by detergent extraction conditions. *J. Neurochem* **82**, 1-5
8. Levine, D. J., Stöhr, J., Falese, L. E., Ollesch, J., Wille, H., Prusiner, S. B., and Long, J. R. (2015) Mechanism of scrapie prion precipitation with phosphotungstate anions. *ACS Chem Biol* **10**, 1269-1277
9. Collinge, J. (2016) Ex vivo mammalian prions are formed of paired double helical prion protein fibrils. *Open Biol 160035* **6**
10. Bode, D. C., Freeley, M., Nield, J., Palma, M., and H., J. (2019) Amyloid-β oligomers have a profound detergent-like effect on lipid membrane bilayers, imaged by atomic force and electron microscopy. *J. Biol.Chem* **294**, 7566-7572
11. Gursky, O. (2015) Role of lipids in protein misfolding. *Adv Exp Med Biol* **855**, v-vii
12. Korshavn, K. J., Satriano, C., Lin, Y., Zhang, R., Dulchavsky, M., Bhunia, A., Ivanova, M. I., Lee, Y.-H., La Rosa, C., Lim, M. H., and Ramamoorthy, A. (2017) Reduced Lipid Bilayer Thickness Regulates the Aggregation and Cytotoxicity of Amyloid-β. *J. Biol.Chem* **292**, 4638-4650
13. Wang, F., and Ma, J. (2013) Role of lipid in forming an infectious prion? *Acta Biochim Biophys* **45**, 485-493
14. Ambadi Thody, S., Mathew, M. K., and Udgaonkar, J. B. (2018) Mechanism of aggregation and membrane interactions of mammalian prion protein. *Biochim Biophys Acta- Biomembr* **1860**, 1927-1935
15. Ambadi Thody, S., Mathew, M. K., and Udgaonkar, J. B. (2018) Mechanism of aggregation and membrane interactions of mammalian prion protein. *Biochim Biophys Acta - Biomembr* **1860**, 1927-1935
16. Dorr, J. M., Scheidelaar, S., Koorengevel, M. C., Dominguez, J. J., Schafer, M., van Walree, C. A., and Killian, J. A. (2016) The styrene-maleic acid copolymer: a versatile tool in membrane research. *Eur Biophys J* **45**, 3-21
17. Knowles, T. J., Scott-Tucker, A., Overduin, M., and Henderson, I. R. (2009) Membrane protein architects: the role of the BAM complex in outer membrane protein assembly. *Nat. Rev. Microbiol* **7**, 206-214
18. Lee, S. C., Knowles, T. J., Postis, V. L. G., Jamshad, M., Parslow, R. A., Lin, Y.-p., Goldman, A., Sridhar, P., Overduin, M., Muench, S. P., and Dafforn, T. R. (2016) A method for detergent-free isolation of membrane proteins in their

Downloaded from http://www.jbc.org/ at University of Alberta Libraries on May 28, 2020

local lipid environment. *Nat. Protoc* **11**, 1149-1162
19. Qiu, W. (2018) Structure and activity of lipid bilayer within a membrane-protein transporter. *Proc Natl Acad Sci U. S. A.* **115**, 12985-12990
20. Sun, C., Benlekbir, S., Venkatakrishnan, P., Wang, Y., Hong, S., Hosler, J., Tajkhorshid, E., Rubinstein, J. L., and Gennis, R. B. (2018) Structure of the alternative complex III in a supercomplex with cytochrome oxidase. *Nature* **557**, 123-126
21. Grethen, A., Oluwole, A. O., Danielczak, B., Vargas, C., and Keller, S. (2017) Thermodynamics of nanodisc formation mediated by styrene/maleic acid (2:1) copolymer. *Sci Rep* **7**, 11517
22. Korotych, O., Mondal, J., Asfura, K. M., Hendricks, J., D., B., and Polym, J. (2018) Evaluation of commercially available styrene-co-maleic acid polymers for the extraction of membrane proteins from spinach chloroplast thylakoids. *Eur. Polym. J* **114**, 485-500
23. Morrison, K. A., Akram, A., Mathews, A., Khan, Z. A., Patel, J. H., Zhou, C., Hardy, D. J., Moore-Kelly, C., Patel, R., Odiba, V., Knowles, T. J., Javed, M.-U.-H., Chmel, N. P., Dafforn, T. R., and Rothnie, A. J. (2016) Membrane protein extraction and purification using styrene-maleic acid (SMA) copolymer: effect of variations in polymer structure. *Biochem J* **473**, 4349-4360
24. Overduin, M. a. E. M. (2019) Native Nanodiscs and the Convergence of Lipidomics, Metabolomics, Interactomics and Proteomics. *Appl. Sci* **9**, 1230
25. D'Castro, L., Wenborn, A., Gros, N., Joiner, S., Cronier, S., Collinge, J., and Wadsworth, J. D. F. (2010) Isolation of proteinase K-sensitive prions using pronase E and phosphotungstic acid. *PLoS ONE* **5**, e15679
26. Priola, S. A., and McNally, K. L. (2009) The role of the prion protein membrane anchor in prion infection. *Prion* **3**, 134-138
27. Wille, H., and Prusiner, S. B. (1999) Ultrastructural studies on scrapie prion protein crystals obtained from reverse micellar solutions. *Biophys. J* **76**, 1048-1062
28. Wille, H., Michelitsch, M. D., Guenebaut, V., Supattapone, S., Serban, A., Cohen, F. E., Agard, D. A., and Prusiner, S. B. (2002) Structural studies of the scrapie prion protein by electron crystallography. *Proc Natl Acad Sci U. S. A.* **99**, 3563-3568
29. Wille, H., Shanmugam, M., Murugesu, M., Ollesch, J., Stubbs, G., Long, J. R., Safar, J. G., and Prusiner, S. B. (2009) Surface charge of polyoxometalates modulates polymerization of the scrapie prion protein. *Proc Natl Acad Sci U. S. A.* **106**, 3740-3745
30. Fantini, J., Garmy, N., Mahfoud, R., and Yahi, N. (2002) Lipid rafts: structure, function and role in HIV, Alzheimer's and prion diseases. *Expert Rev Mol Med* **4**, 1-22
31. Taylor, D. R., and Hooper, N. M. (2006) The prion protein and lipid rafts. *Mol. Membr. Biol* **23**, 89-99
32. Camargo, M., Intasqui Lopes, P., Del Giudice, P. T., Carvalho, V. M., Cardozo, K. H. M., Andreoni, C., Fraietta, R., and Bertolla, R. P. (2013) Unbiased label-free quantitative proteomic profiling and enriched proteomic pathways in seminal plasma of adult men before and after varicocelectomy. *Hum. Reprod* **28**, 33-46
33. Sciacca, M. F. M., Tempra, C., Scollo, F., and Milardi D, L. R. C. (2018) Amyloid growth and membrane damage: Current themes and emerging perspectives from theory and experiments on Aβ and hIAPP. *Biochim Biophys Acta-Biomembr* **1860**, 1625-1638
34. Klein, T. R., Kirsch, D., Kaufmann, R., and Riesner, D. (1998) Prion rods contain small amounts of two host sphingolipids as revealed by thin-layer chromatography and mass spectrometry. *Biol. Chem* **379**, 655-666
35. Simons, K., and Toomre, D. (2000) Lipid rafts and signal transduction. *Nat. Rev. Mol. Cell Biol* **1**, 31-39

Downloaded from http://www.jbc.org/ at University of Alberta Libraries on May 28, 2020

36. Guo, B. B., Bellingham, S. A., and Hill, A. F. (2015) The neutral sphingomyelinase pathway regulates packaging of the prion protein into exosomes. *J. Biol.Chem* **290**, 3455-3467
37. Hannun, Y. A., and Obeid, L. M. (2008) Principles of bioactive lipid signalling: lessons from sphingolipids. *Nat. Rev. Mol. Cell Biol* **9**, 139-150
38. Gonzalez-Romero, D., Barria, M. A., Leon, P., Morales, R., and Soto, C. (2008) Detection of infectious prions in urine. *FEBS Lett* **582**, 3161-3166
39. Cronier, S., Gros, N., Tattum, M. H., Jackson, G. S., Clarke, A. R., Collinge, J., and Wadsworth, J. D. F. (2008) Detection and characterization of proteinase K-sensitive disease-related prion protein with thermolysin. *Biochem. J* **416**, 297-305
40. Angelisová, P., Ballek, O., Sýkora, J., Benada, O., Čajka, T., Pokorná, J., Pinkas, D., and Hořejší, V. (2019) The use of styrene-maleic acid copolymer (SMA) for studies on T cell membrane rafts. *Biochim Biophys Acta-Biomembr* **1861**, 130-141
41. Falcon, B., Zivanov, J., Zhang, W., Murzin, A. G., Garringer, H. J., Vidal, R., Crowther, R. A., Newell, K. L., Ghetti, B., Goedert, M., and Scheres, S. H. W. (2019) Novel tau filament fold in chronic traumatic encephalopathy encloses hydrophobic molecules. *Nature* **568**, 420-423
42. Teruya, K., Oguma, A., Nishizawa, K., Kawata, M., Sakasegawa, Y., Kamitakahara, H., and Doh-Ura, K. (2016) A Single Subcutaneous Injection of Cellulose Ethers Administered Long before Infection Confers Sustained Protection against Prion Diseases in Rodents. *PLoS Pathog* **12**, e1006045
43. Tonge, S. R., and Tighe, B. J. (2001) Responsive hydrophobically associating polymers: a review of structure and properties. *Adv. Drug Deliv. Rev* **53**, 109-122
44. Tsukigawa, K., Liao, L., Nakamura, H., Fang, J., Greish, K., Otagiri, M., and Maeda, H. (2015) Synthesis and therapeutic effect of styrene-maleic acid copolymer-conjugated pirarubicin. *Cancer Sci* **106**, 270-278
45. McCarthy, J. M., Rasines Moreno, B., Filippini, D., Komber, H., Maly, M., Cernescu, M., Brutschy, B., Appelhans, D., and Rogers, M. S. (2013) Influence of surface groups on poly(propylene imine) dendrimers antiprion activity. *Biomacromolecules* **14**, 27-37
46. Beom Lim, Yong, E., M. C., Younghwan, K., B., T. W., and Chongsuk, R. (2010) The inhibition of prions through blocking prion conversion by permanently charged branched polyamines of low cytotoxicity. *Biomaterials* **31**, 2025-2033
47. Fischer, M., Appelhans, D., Schwarz, S., Klajnert, B., Bryszewska, M., Voit, B., and Rogers, M. (2010) Influence of surface functionality of poly(propylene imine) dendrimers on protease resistance and propagation of the scrapie prion protein. *Biomacromolecules* **11**, 1314-1325
48. Supattapone, S., Nguyen, H. O., Cohen, F. E., Prusiner, S. B., and Scott, M. R. (1999) Elimination of prions by branched polyamines and implications for therapeutics. *Proc Natl Acad Sci U. S. A.* **96**, 14529-14534
49. Lindhoud, S., Carvalho, V., Pronk, J. W., and Aubin-Tam, M. E. (2016) SMA-SH: Modified Styrene-Maleic Acid Copolymer for Functionalization of Lipid Nanodiscs. *Biomacromolecules* **17**, 1516-1522
50. Wenborn, A., Terry, C., Gros, N., Joiner, S., D'Castro, L., Panico, S., Sells, J., Cronier, S., Linehan, J. M., Brandner, S., Saibil, H. R., Collinge, J., and Wadsworth, J. D. (2015) A novel and rapid method for obtaining high titre intact prion strains from mammalian brain. *Sci Rep* **5**, 10062
51. Dorr, J. M., Koorengevel, M. C., Schafer, M., Prokofyev, A. V., Scheidelaar, S., van der Cruijsen, E. A., Dafforn, T. R., Baldus, M., and Killian, J. A. (2014) Detergent-free isolation, characterization, and functional

Downloaded from http://www.jbc.org/ at University of Alberta Libraries on May 28, 2020

reconstitution of a tetrameric K+ channel: the power of native nanodiscs. *Proc Natl Acad Sci U. S. A.* **111**, 18607-18612

52. Botsios, S., Tittman, S., and Manuelidis, L. (2015) Rapid chemical decontamination of infectious CJD and scrapie particles parallels treatments known to disrupt microbes and biofilms. *Virulence* **6**, 787-801

53. Graeve, M., and Janssen, D. (2009) Improved separation and quantification of neutral and polar lipid classes by HPLC-ELSD using a monolithic silica phase: application to exceptional marine lipids. *J Chromatogr B Analyt Technol Biomed Life Sci* **877**, 1815-1819

Downloaded from http://www.jbc.org/ at University of Alberta Libraries on May 28, 2020

TABLES

A

Sample	Incubation period (days) ± SEM (N/N_0)
1% 263K brain homogenate (control)	71±0.5 (4/4)
treated with 1% Sarkosyl-PrP^{Sc} (control)	76±5 (12/12)
treated with 1% SMA(1:1)ma-PrP^{Sc}	84±8 (12/12)
treated with 1% SMA(2:1)-PrP^{Sc}	87±3 (12/12)
treated with 1% SMA-SH-PrP^{Sc}	88±4 (12/12)*
treated with 1% SMA(3:1)-PrP^{Sc}	94±3 (12/12)*

B

Sample	Incubation period (days) ± SEM (N/N_0)
treated with 1% Sarkosyl-PrP^{Sc} (control)	158±19 (19/19)
treated with 1% SMA(1:1)ma-PrP^{Sc}	174±27 (9/9)
treated with 1% SMA(2:1)-PrP^{Sc}	172±21 (15/15)
treated with 1% SMA-SH-PrP^{Sc}	163±15 (14/14)
treated with 1% SMA(3:1)-PrP^{Sc}	187±33.5 (17/17)*

Table 1. A summary of the infectivity of SMA-treated PrP^{Sc} samples in samples from Hyper-infected hamsters (*A*) and RML-infected mice (B). In both cases, 10% brain homogenates and Sarkosyl purified PrP^{Sc} were used as controls. Asterisks indicate the significant difference (P-value < 0.001) between the incubation periods of SMA-treated samples and sarkosyl-purified PrP^{Sc}.

Re-inoculation Sample (Hamster)	Incubation period (days) ± SEM (N/N_0)
1% 263K brain homogenate (control)	71±0.5 (4/4)
treated with 1% SMA(1:1)ma-PrP^{Sc}	87±3 (10/10)*
treated with 1% SMA(2:1)-PrP^{Sc}	74±3 (6/6)
treated with 1% SMA-SH-PrP^{Sc}	97±2 (6/6)*
treated with 1% SMA(3:1)-PrP^{Sc}	115±0.5 (6/6)*

Table 2. The second passage of brain homogenates of animals infected with SMA-isolated-Hyper PrP^{Sc} into healthy Syrian hamsters. Asterisks indicate the significant difference (P-value < 0.001) between the incubation periods of SMA-treated samples and the control. The largest differences were in SMA-SH-PrP^{Sc} and SMA(3:1)- PrP^{Sc}, as seen in the first passage (Table 1).

Downloaded from http://www.jbc.org/ at University of Alberta Libraries on May 28, 2020

FIGURE LEGENDS

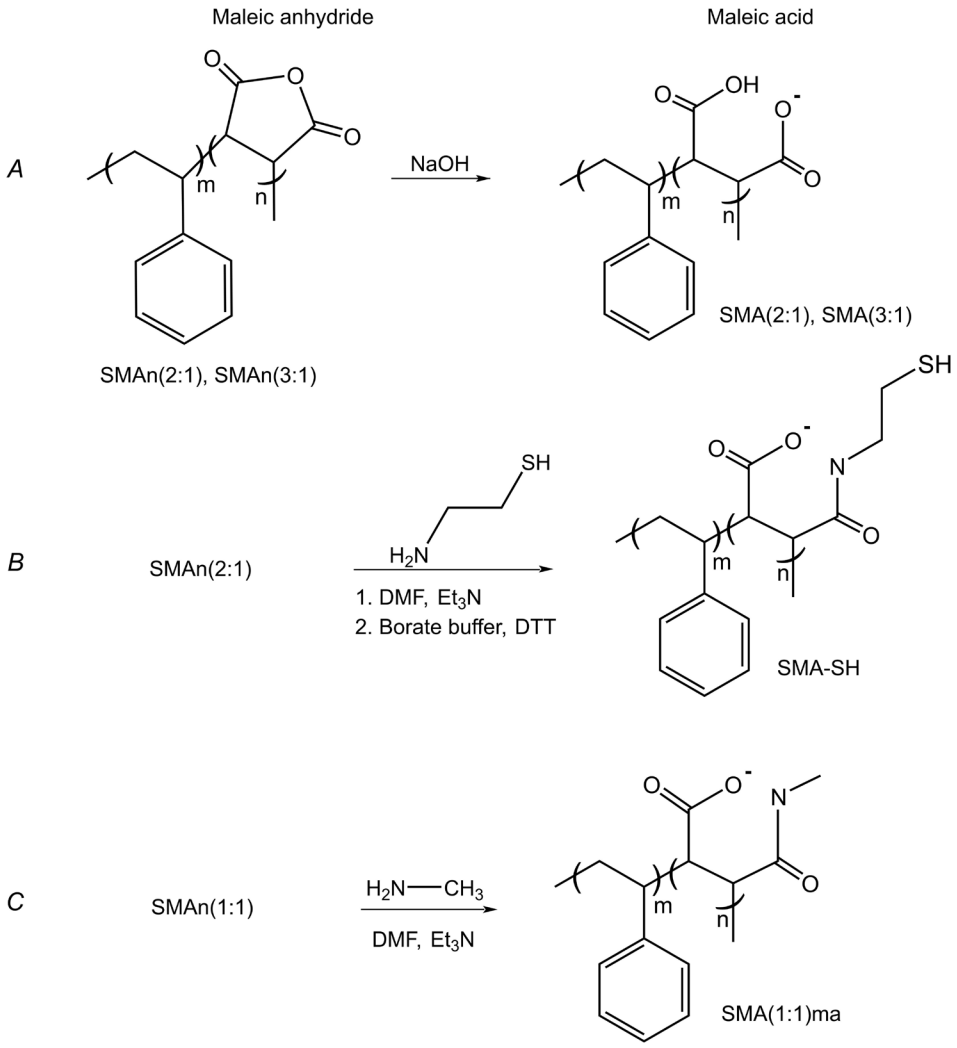

Fig. 1. Chemical structures and synthesis of the (*A*) SMA(2:1), SMA(3:1) (*B*) SMA-SH and (*C*) SMA(1:1)ma copolymers, which have average m:n ratios of styrene to maleic acid groups of 2:1, 3:1, 2:1 and 1:1, respectively.

Downloaded from http://www.jbc.org/ at University of Alberta Libraries on May 28, 2020

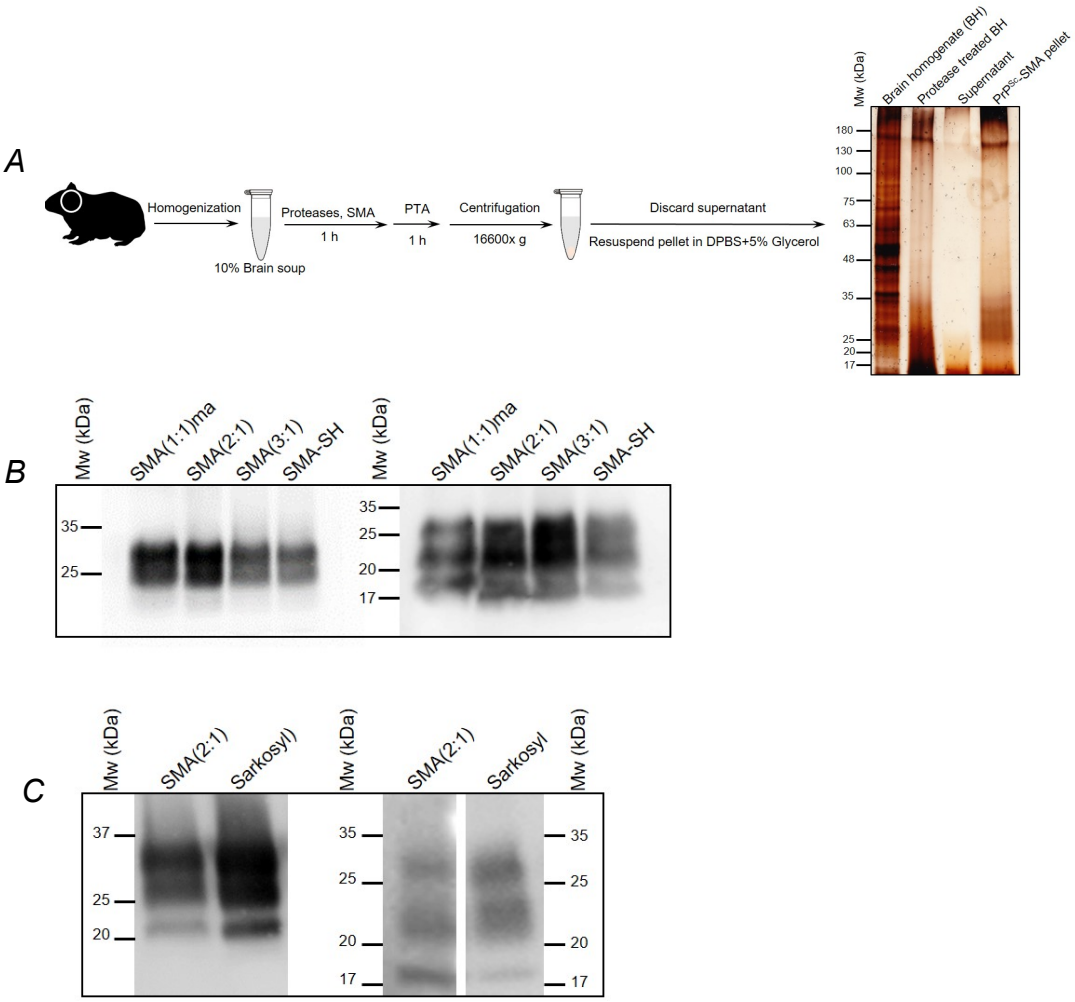

Fig. 2. (*A*) Schematic description of detergent-free isolation of protease-resistant prions from infected brain tissues. (*B*) Immunoblots of SMA-purified PrP^{Sc} from Hyper-infected Syrian hamsters (left) and RML-infected wild-type mice (right) using anti-PrP primary antibody, showing similar molecular weights and glycosylation patterns for the SMA-purified PrP^{Sc} preparation compared to samples purified with sarkosyl. (*C*) Comparison between glycosylation patterns of sarkosyl-purified and SMA(2:1)- isolated PrP^{Sc} derived from Hyper infected Syrian hamster (left) and RML-infected wild-type mice (right).

Downloaded from http://www.jbc.org/ at University of Alberta Libraries on May 28, 2020

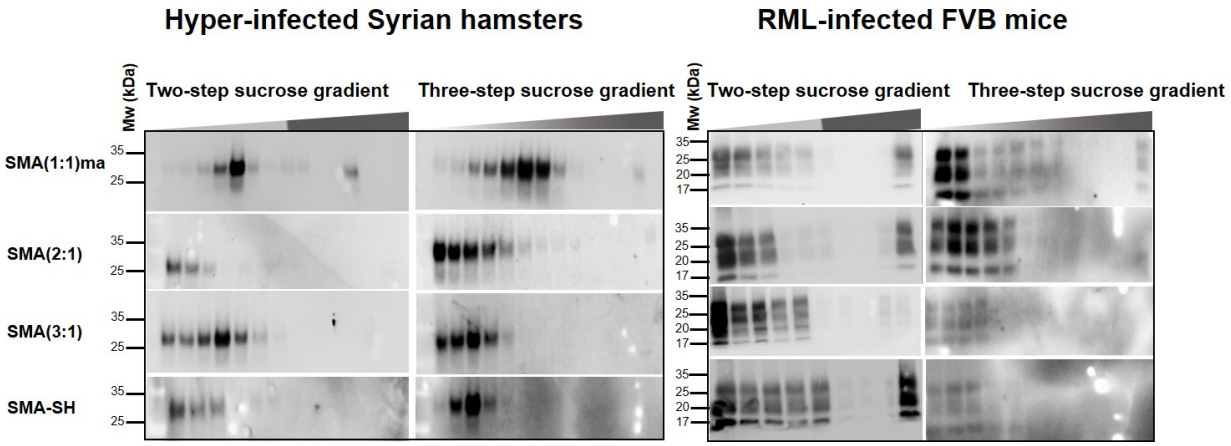

Fig. 3. Protease treated SMA-PrP^{Sc} particles isolated from Hyper-infected Syrian hamsters and RML-infected FVB mice were separated according to their densities using two-step (40 and 80%) and three-step (40, 55 and 80%) sucrose gradient ultracentrifugations, with fractions collected from the top to the bottom of tubes for immunoblotting. The majority of prion particles remained in the top layer of the gradient (40%), implying less aggregated, lipid-bound states of PrP^{Sc} in SMA nanodiscs.

Downloaded from http://www.jbc.org/ at University of Alberta Libraries on May 28, 2020

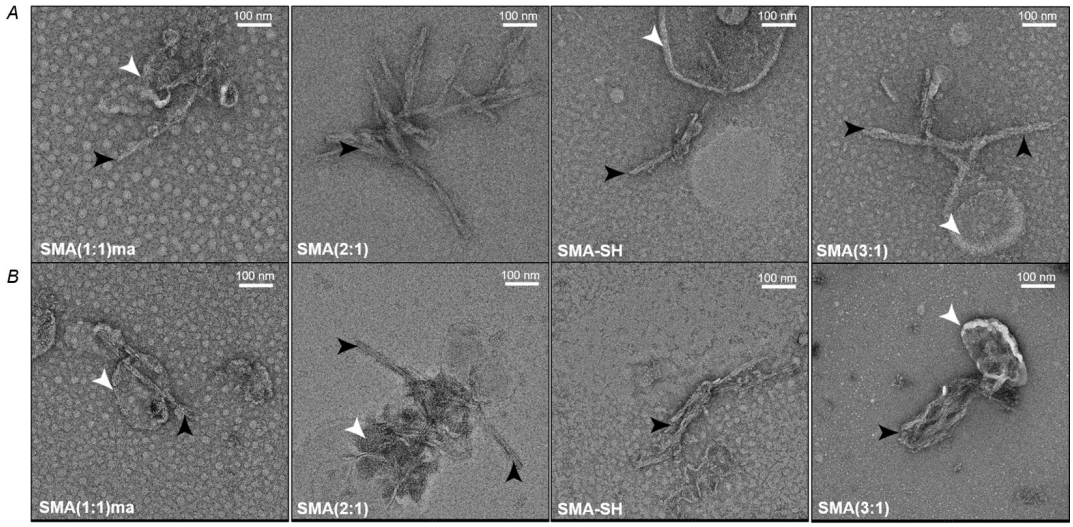

Fig. 4. Negative stain electron micrographs of PrP^{Sc} fibrils from Hyper-infected Syrian hamsters (*A*) and RML-infected wild-type mice (*B*) using the indicated SMA copolymers. Black arrows point to isolated PrP^{Sc} fibrils and white arrows highlight the co-purified lipid vesicles.

Downloaded from http://www.jbc.org/ at University of Alberta Libraries on May 28, 2020

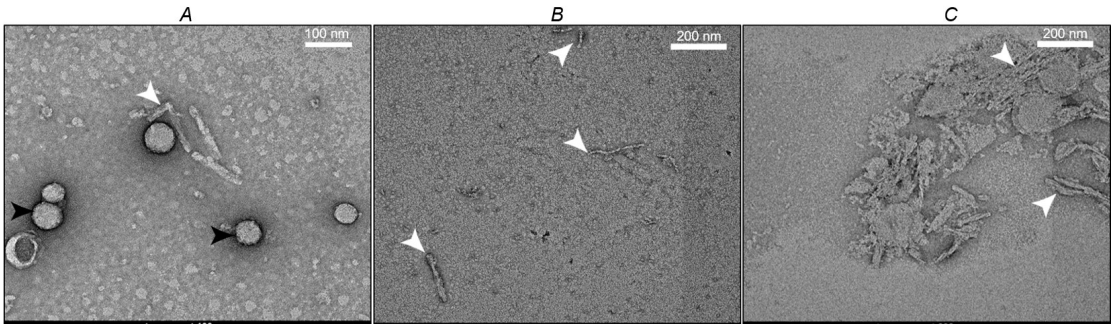

Fig. 5. Negative stained electron micrographs of (*A*) PrP^{Sc} fibrils (white arrow) and small 2D crystals from Hyper-infected Syrian hamster following SMA-SH and PK-treatment (black arrow). Protofilaments and vesicle from the top-most fractions of sucrose gradients of SMA(2:1) (*B*) and SMA(1:1)ma (*C*)-treated Hyper-infected hamster brain.

Downloaded from http://www.jbc.org/ at University of Alberta Libraries on May 28, 2020

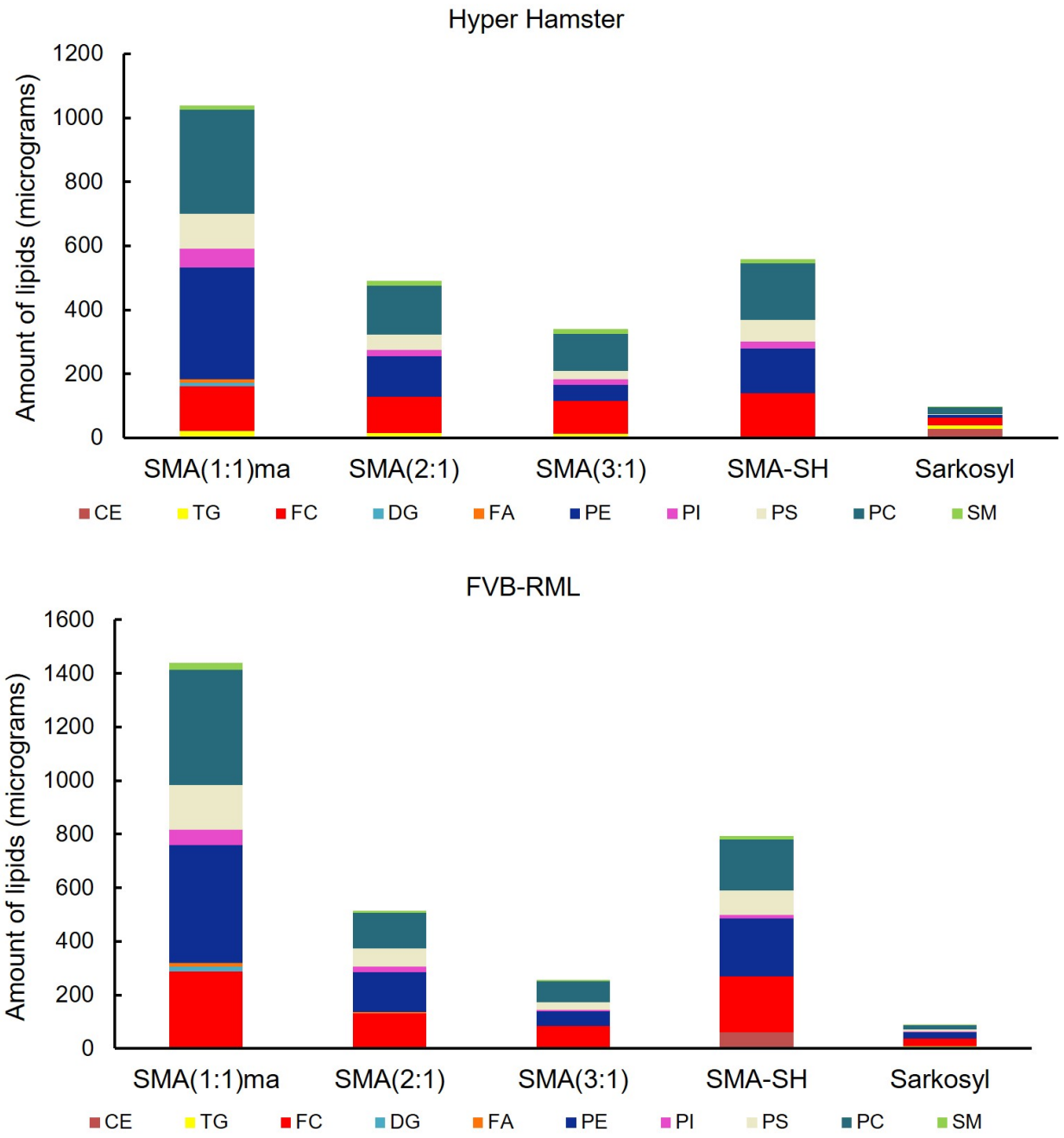

Fig. 6. Different lipid species in each SMA isolated-PrP^{Sc} pellet from Hyper-infected hamster (above) and RML-infected wild-type mice (below) were quantified and their cumulative amounts shown in stack plots including levels of cholesteryl esters (CE1 and CE2), triacylglycerol (TG), free cholesterol (FC), diacylglycerol (DG), free fatty acid (FA), phosphatidylethanolamine (PE), phosphatidylinositol (PI), phosphatidylserine (PS), phosphatidylcholine (PC) and sphingomyelin (SM).

Downloaded from http://www.jbc.org/ at University of Alberta Libraries on May 28, 2020

Downloaded from http://www.jbc.org/ at University of Alberta Libraries on May 28, 2020

Native nanodiscs formed by styrene-maleic acid copolymer derivatives help recover infectious prion multimers bound to brain-derived lipids

Mansoore Esmaili, Brian P Tancowny, Xiongyao Wang, Audric Moses, Leonardo Cortez, Valerie Sim, Holger Wille and Michael Overduin

J. Biol. Chem. published online May 1, 2020

Access the most updated version of this article at doi: 10.1074/jbc.RA119.012348

Alerts:
- When this article is cited
- When a correction for this article is posted

Click here to choose from all of JBC's e-mail alerts

Downloaded from http://www.jbc.org/ at University of Alberta Libraries on May 28, 2020